IMPULSIVE NOISE REMOVING WITH VECTOR MEDIAN FILTERS: A DETERMINISTIC APPROACH

Laurent LUCAT and Pierre SIOHAN

France Telecom - CNET/DSM, CCETT Laboratory
4, Rue du Clos Courtel, 35512 Cesson-Sévigné Cédex, FRANCE
E-mail : laurent.lucat@cnet.francetelecom.fr

ABSTRACT

Vector Median (VM) filters are known to globally perform better than scalar independent median filters around edges. In this work, we examine the filtering of vector edges corrupted by scalar impulsive noise. We show that VM performance is highly dependent on the relative magnitude of the impulses, the noisy component and the noise-free components of the edges. This characteristic gives some indications for adequately choosing the norm (L_1/L_2) of the VM filter and the standard (RGB/YUV) of data representation.

1. INTRODUCTION

Scalar median filtering is known to produce artifacts when applied independently to all channels of a multi-component (vector) signal. Such artifacts can be observed around edges, when filtering a color image embedded in an impulsive noise. In order to take advantage of the particularity of multi-component signals, vector median (VM) filters have been introduced [1]. Simulations have shown that VM filtering can partly avoid these artifacts of the scalar independent median, also called "marginal median" (mm) filter [2], but a theoretical proof has not yet been given. Some statistical results are presented in [1] and [3], but the considered input signal is always a constant vector corrupted by additive noise, and in this case, mm filter is often preferable to VM filter. Since experiments indicate that, on noisy edges, VM can work better than mm filters, it is of great interest to theoretically compare mm and VM filter outputs, when the filter's input is a noisy edge. Such an approach was also used in [4]. Median type filtering being well suited for "heavy-tailed" noise, we also consider edges corrupted by impulsive noise.

After some further precisions about the considered input signal, in Section 2 we express the output of the VM filter, defined with both the L_1 norm (leading to the VML_1 filter) and the L_2 norm (VML_2 filter), as a function of the impulse magnitude, with respect to that of the edge components. These results will be illustrated in Section 3 using a synthetic pattern of vector edges. A comparison of mm and VM filters is also presented in Section 4 with color natural images, both in the RGB (Red, Green, Blue) and YUV (Luminance and Chrominance) standards.

2. THEORETICAL ANALYSIS

2.1. Assumptions of our model and simplifications

• We consider a vector signal consisting of a vector edge affected by a scalar impulse. *Vector edge* means that the components of the edge are located at the same spatial position for each component; however, the magnitude of the edge can be different on each vector component.

• This model leads to 4 possible configurations for the "noisy component", that is the signal component containing the impulse, as depicted in Fig. 1.
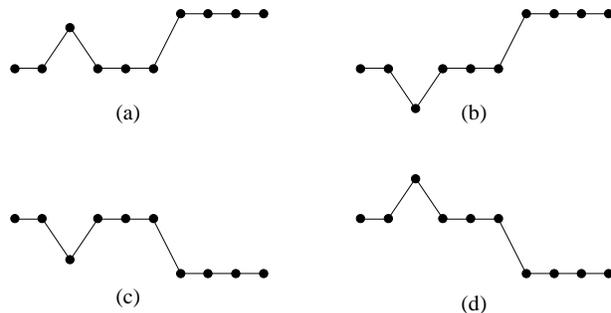

Figure 1: 4 configurations for the impulse and the edge.

It can be seen that the configuration (a) is analogous to (c), as well as (b) is analogous to (d). Hence, we can confine our analysis to the (a) and (b) configurations.

• Let $W = 2N + 1$ be the window's size. If the window is not centered on the edge, as for the example in Fig. 2 (using one-dimensional data and W=5), there are at least $N + 2$ samples equal to a same value we denote X, if no impulse is present, and there are at least $N + 1$ samples equal to X in the presence of one impulse, no matter where this impulse is located.

So, in the case of an "uncentered window", the output of the filters (mm, VML_1 and VML_2) is always equal to this value X. The only window position we have to consider in the following also corresponds to the "central position" (window centered on the edge).

• The edge can be either ascending or descending on the "impulse-free" components; this does not affect the analysis
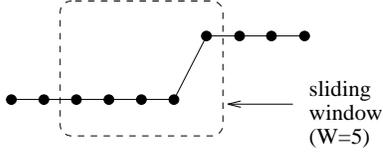
Figure 2: Example of a window being uncentered on the edge.

of the mm, VML_1 and VML_2 filter output.

In conclusion, without loss of generality, it is sufficient to analyze the output of the mm, VML_1 and VML_2 filters to a vector edge, ascendant on its noisy component, where the scalar impulse (which can be either positive or negative) affects a sample of the low level, and where the sliding window is centered on the edge, as it is summarized in Fig. 3. The only constrainst of our model is that there is no more than one impulse in the window, which is a realistic assumption when the probability of impulse occurence is not too high.
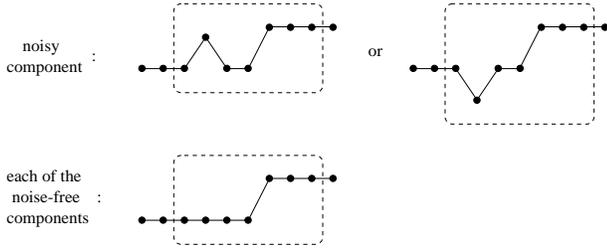

Figure 3: Configuration to be studied (magnitude of each edge component and of the impulse are variable).

2.2. Principle of the analysis

According to the simplifications mentioned in section §2.1, the samples included in the window can be split in 3 classes : there are N vector samples corresponding to the low edge level, denoted (1), N vector samples of the high edge level, denoted (2), and one vector sample corrupted by a scalar impulse, denoted (i).

The vector median filter is defined as [1]

$$y_{VML_p} = \arg \min_{x_l \in W} \sum_{j=1}^{2N+1} \|x_l - x_j\|_{L_p}, \qquad (1)$$

where L_p is the considered norm (L_1 or L_2).
In our case, $\arg \min_{x_l \in W} (.)$ is one of the 3 vectors (1), (2) or (i). The VM filter can be rewritten as:

$$y_{VML_p} = \arg \min_{(1),(2),(i)} (d_1, d_2, d_i), \qquad (2)$$

where

$$\begin{cases} d_1 & = \sum_{j=1}^{2N+1} \|(1) - x_j\|_{L_p} & = N d_{12} + d_{1i} \\ d_2 & = \sum_{j=1}^{2N+1} \|(2) - x_j\|_{L_p} & = N d_{12} + d_{2i} \qquad (3) \\ d_i & = \sum_{j=1}^{2N+1} \|(i) - x_j\|_{L_p} & = N(d_{1i} + d_{2i}) \end{cases}$$

with: $d_{12} = \|(2) - (1)\|_{L_p}$, $d_{1i} = \|(1) - (i)\|_{L_p}$ and $d_{2i} = \|(2) - (i)\|_{L_p}$.

Using this notation, the VM filter's output can be expressed as

$$y_{VML_p} = \begin{cases} (1) & \text{if} \begin{cases} d_1 < d_2 \\ d_1 < d_i \end{cases} \\ (2) & \text{if} \begin{cases} d_2 < d_1 \\ d_2 < d_i \end{cases} \qquad (4) \\ (i) & \text{if} \begin{cases} d_i < d_1 \\ d_i < d_2 \end{cases} \end{cases}$$

When d_1, d_2 or d_i are equal, an additional rule is required to determine the VM filter's output. This particular case is not of interest for our analysis and will be later ignored.

2.3. The VML_1 filtering

Theoretical analysis of the VM filter, using L_1 metric, can be split in 3 cases, according to the magnitude of the impulse. In the following, Δ denotes the magnitude of the noisy edge component.

2.3.1. Negative impulse

In Fig. 4, we represent the $2N+1$ vectors in a two-dimensional space (X,Y), where the negative impulse affects the component Y of a vector (1).
Using the L_1 metric, $d_{2i} = d_{12} + d_{1i}$, which involves $d_{2i} > d_{1i}$. Combining this with equation (3), we get

- $d_2 > d_1$,
- $d_i = N d_{12} + 2N d_{1i} > d_1$.

So, according to eq. (4), the output of the VML_1 filter corresponds to vector (1).

2.3.2. Positive impulse whose level is lower than Δ

This configuration is illustrated in Fig. 5 for two-dimensional data. In this case, $d_{12} = d_{1i} + d_{2i}$. Substituting in eq. (3), we get

- $d_1 = N(d_{1i} + d_{2i}) + d_{1i} > d_i$,
- $d_2 = N(d_{1i} + d_{2i}) + d_{2i} > d_i$.

Hence, the output of the VML_1 filter corresponds to the impulse (i).
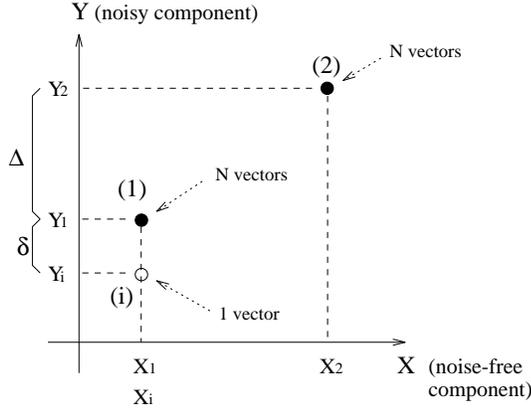
Figure 4: Input vectors in the 2-dimensional space (X,Y), with a negative impulse.
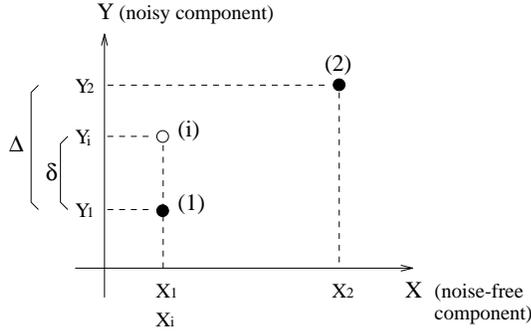
Figure 5: Input vectors, with a positive impulse whose magnitude is lower than the noisy edge component.

2.3.3. *Positive impulse with a level greater than Δ*

The corresponding case is reported in Fig. 6, for two-dimensional data. We then get $d_{1i} = \Delta + \delta$ and $d_{2i} = d_{12} - \Delta + \delta$, leading to

$$\left\{ \begin{array}{ll} d_1 & = Nd_{12} + \Delta + \delta, \\ d_2 & = (N+1)d_{12} - \Delta + \delta, \\ d_i & = Nd_{12} + 2N\delta. \end{array} \right.$$

Thus,

- $d_1 < d_2 \quad \Leftrightarrow \Delta < \frac{d_{12}}{2}$,
- $d_1 < d_i \quad \Leftrightarrow \delta > \frac{\Delta}{2N-1}$,
- $d_2 < d_i \quad \Leftrightarrow \delta > \frac{d_{12}-\Delta}{2N-1}$.

The output of the VML_1 filter is therefore given by

$$\left\{ \begin{array}{l} \text{if } \Delta < \frac{d_{12}}{2} : y_{VML_1} = \left\{ \begin{array}{ll} (i) & \text{if } \delta < \frac{\Delta}{2N-1} \\ (1) & \text{otherwise} \end{array} \right. , \\ \\ \text{if } \Delta > \frac{d_{12}}{2} : y_{VML_1} = \left\{ \begin{array}{ll} (i) & \text{if } \delta < \frac{d_{12}-\Delta}{2N-1} \\ (2) & \text{otherwise} \end{array} \right. . \end{array} \right.$$
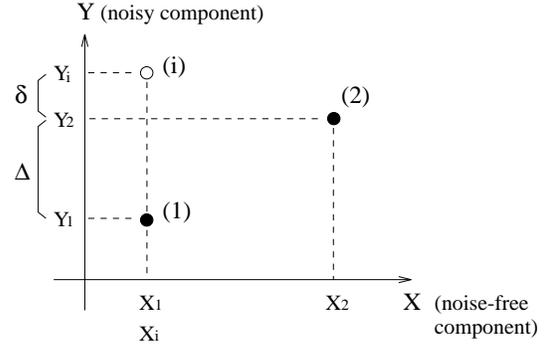
Figure 6: Input vectors, with a positive impulse whose magnitude is greater than the edge noisy component.

2.4. The VML_2 filtering

According to our model of signal and noise, VML_2 filtering is based on eq. (3) and (4), where the distances are computed using L_2 metric. The analysis can be again split in 3 cases.

Let us define γ as the magnitude (L_2) of the edge without its noisy component, so as $\Delta^2 + \gamma^2 = d_{12}^2$.

2.4.1. *Negative impulse*

We refer to Fig. 4. Using L_2 metric, we get

- $d_{2i} = \sqrt{\gamma^2 + (\Delta + \delta)^2} > \delta$, so $d_{2i} > d_{1i}$. According to eq. (3), we obtain $d_2 > d_1$.
- $d_i = Nd_{1i} + N\sqrt{\gamma^2 + (\Delta + \delta)^2} > Nd_{12} + d_{1i}$, which involves $d_i > d_1$.

Thus, according to eq. (4), the output of the VML_2 filter is the vector (1).

2.4.2. *Positive impulse, with $0 < \delta < \Delta$*

We, now, refer to Fig. 5. The use of L_2 metric leads to

$$\left\{ \begin{array}{l} d_{1i} = \delta, \\ d_{2i} = \sqrt{\gamma^2 + (\Delta - \delta)^2}. \end{array} \right.$$

Substituting into eq. (3),

- $d_i < d_1 \quad \Leftrightarrow \quad \delta < 2\dfrac{\Delta - kd_{12}}{1 - k^2}, \text{ with } k = \dfrac{N-1}{N}$
- $d_i < d_2 \quad \Leftrightarrow \quad \delta < \delta_1$ (5)

where $\delta_1 = \dfrac{d_{12} - k^2\Delta - k\sqrt{2d_{12}^2 - 2\Delta d_{12} - k^2\gamma^2}}{1 - k^2}$ (proof of (5) is given in the appendix).

- $d_2 < d_1 \Leftrightarrow \delta > \dfrac{d_{12}^2}{2\Delta}$

  * if $\gamma > \Delta$, which is equivalent to $d_{12} > \sqrt{2}\Delta$, then $\frac{d_{12}^2}{2\Delta} > \Delta$; the inequality $\delta > \frac{d_{12}^2}{2\Delta}$ becomes impossible (contrary to the hypothesis of §2.4.2). Thus, $d_1 < d_2$, and we get

$$y_{VML_2} = \begin{cases} (i) & \text{if } \delta < 2\frac{\Delta - kd_{12}}{1-k^2} \\ (1) & \text{otherwise} \end{cases} \quad .$$

* case where $\gamma < \Delta$: the output of the VML_2 is given by

$$y_{VML_2} = \begin{cases} (i) & \text{if } \delta < 2\frac{\Delta - kd_{12}}{1-k^2} \\ \\ (1) & \text{if } 2\frac{\Delta - kd_{12}}{1-k^2} < \delta < \frac{d_{12}^2}{2\Delta} \\ \\ (2) & \text{if } \delta > \frac{d_{12}^2}{2\Delta} \end{cases} \quad .$$

2.4.3. <u>Positive impulse, with a level greater than Δ</u>

A two-dimensional representation is given in Fig. 6. We have

$$\begin{cases} d_{1i} = \Delta + \delta \\ d_{2i} = \sqrt{\gamma^2 + \delta^2} \end{cases} \quad .$$

• It can be shown that d_i is always greater than d_1. The filter's output is then (1) or (2).

• $d_1 < d_2 \Leftrightarrow \delta < \frac{\gamma^2 - \Delta^2}{2\Delta}$. Thus,

  * if $\gamma < \Delta$, $d_2 < d_1$, that is $y_{VML_2} = (2)$

  * if $\gamma > \Delta$, $y_{VML_2} = \begin{cases} (1) & \text{if } \delta < \frac{\gamma^2 - \Delta^2}{2\Delta} \\ (2) & \text{otherwise} \end{cases} \quad .$

2.5. Schematic synthesis of theoretical analysis

In order to summarize the different configurations we encountered in the analysis, outputs of the VML_1 and VML_2 filters are given in Fig. 7; output of the marginal median is also presented as a matter of comparison. This clearly shows that the output of the filters is highly dependent upon the magnitude of the impulse, with regard to that of the noisy edge component. The different configurations we studied correspond to different relative contributions of the noisy and noise-free components in the global norm of the edge. This point has a practical interest which is discussed in §4. We use the following notations:
$r1+ : \Delta > \frac{d_{12}}{2}$; $r2+ : \Delta > \frac{d_{12}}{\sqrt{2}}$. Conditions "$rl$-" are dual with "$rl+$" ($l = 1, 2$), i.e. the symbol $<$ replaces $>$.
Thresholds are defined as $t_1 = \Delta + \frac{\Delta}{2N-1}$, $t_2 = \Delta + \frac{d_{12}-\Delta}{2N-1}$, $t_3 = \Delta + \frac{\gamma^2 - \Delta^2}{2\Delta}$, $t_4 = \frac{d_{12}^2}{2\Delta}$, $t_5 = 2\frac{\Delta - kd_{12}}{1-k^2}$.

3. ILLUSTRATION USING SYNTHETIC IMAGES

In order to illustrate the results of the precedent theoretical analysis, in Fig. 8 we give comparative outputs of mm, VML_1 and VML_2 filtering, using a 5 pixels horizontal mask. Input signal is an R-G-B test pattern of vertical contours, which are embedded in a channel-independent impulsive noise. The magnitude of these "salt-and-pepper" impulses is increasing when going from the left to the right of the
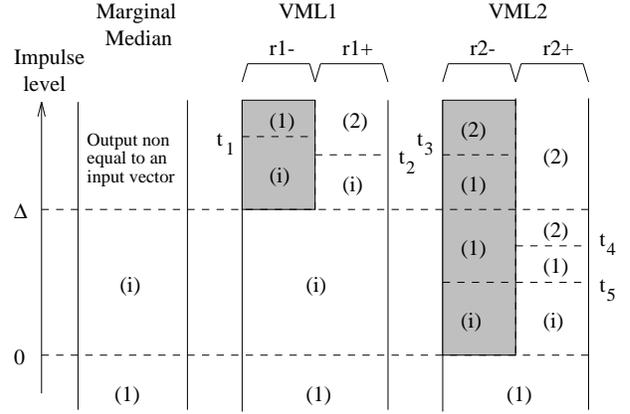

Figure 7: Filter outputs for the marginal and vector median (VML_1, VML_2) filters for an edge, with low level (1) and high level (2), corrupted by an impulse i. (The notation is completely defined in the text.)

test image.
For this particular image, the magnitude of the edges is equal for each signal component, and constant over the image, so that

  * $d_{12} = 3\Delta$, using L_1 norm, leading to the case "r1-" in Fig. 7 (i.e. $\Delta < \frac{d_{12}}{2}$)
  * $d_{12} = \sqrt{3}\Delta$, using L_2 norm, which involves $\Delta < \frac{d_{12}}{\sqrt{2}}$, thus referring to the case "r2-".
These two cases correspond to the grey part in Fig. 7.

Both theoretical and simulation results clearly show the global superiority of VM with regard to mm filtering in this case of edges corrupted by scalar independent impulses. Secondly, the "surprizing" different behaviors of VML_1 and VML_2 filters emphasize the fact that an a priori knowledge of impulse levels could drive the choice of the norm.

4. FILTERING OF COLOR IMAGES

Simulations have also been driven using natural color images. In Fig. 9, we report the results of mm and VM filtering, where the R-G-B input image "boat" is corrupted by channel-independent impulsive noise. This figure is a clear illustration of the global superiority of VM over mm filtering, for R-G-B images corrupted with this kind of degradation, especially when looking at the edges (ropes and hull). The same image, now in the Y-U-V format, is presented in Fig. 10; the 3 components are affected by scalar independent impulses. In this case, the difference between marginal and vector median filtering is weak; this is because artifacts on the edges caused by mm filtering are less sensitive in the Y-U-V standard; another reason is relative to VM filter: edge magnitude on the Y component is often consequently greater than those on U and V channels; so, impulses on Y often correspond to the cases "r1+" and "r2+" of Fig. 7,

which more often produce erroneous output values. Thus, the superiority of VM over mm filtering is especially effective in R-G-B standard.

5. CONCLUSIONS

In this paper, we analyzed the response of the vector median filter (defined with both L_1 and L_2 norm) to vector edges corrupted by channel-independent impulsive noise. In particular, we compared vector median with marginal median filtering, which is known to produce artifacts with this type of input signal. Our theoretical analysis confirms that the vector median globally outperforms the marginal median filter with such input signals. However, this work emphasizes that the filtering performance is highly dependent on input data and on the choice of the norm used for the VM operator. Especially, the relative magnitude between impulses and edges, as well as between edge components, considerably influence the filter's output.

Consequently, a priori knowledge of impulse level, with regard to the input signal, should be a determinant information in the design of the filter (choice of the norm). We also showed that VM filtering works better when edge components have comparable magnitudes; hence, VM is expected to perform better in R-G-B than in Y-U-V standard, where edge magnitude on the Y component is often significantly higher than in other channels. Theoretical results have also been illustrated using synthetic and natural color images.

6. APPENDIX

Mathematical proof of eq. (5):

$$d_i < d_2 \quad \Leftrightarrow \quad \delta^2 + 2\delta \frac{k^2\Delta - d_{12}}{1 - k^2} + d_{12}^2 > 0.$$

Let us define the polynomial $P(\delta)$ as

$$P(\delta) = \delta^2 + \delta \frac{k^2\Delta - d_{12}}{1 - k^2} + d_{12}^2.$$

Reduced discriminant Q of $P(\delta)$ is

$$Q = Q(\Delta) = \frac{(k^2\Delta - d_{12})^2}{(1 - k^2)^2} - d_{12}^2,$$

$$Q(\Delta) > 0 \quad \Leftrightarrow \quad k^2\Delta^2 - 2d_{12}\Delta + (2 - k^2)d_{12}^2 > 0$$
$$\Leftrightarrow \quad Q^{'}(\Delta) > 0,$$

with $Q^{'}(\Delta) = k^2\Delta^2 - 2d_{12}\Delta + (2 - k^2)d_{12}^2$. The two roots of $Q^{'}$ are $\Delta_1 = d_{12}$ and $\Delta_2 = \frac{2 - k^2}{k^2}d_{12}$; thus

$$Q^{'}(\Delta) > 0 \quad \Leftrightarrow \quad \Delta < d_{12} \text{ or } \Delta > \Delta_2.$$

Condition $\Delta < d_{12}$ is always satisfied, so that $Q(\Delta)$ is always positive. Hence, $P(\delta)$ has two roots, δ_1 (as defined in §2.4.2) and δ_2 ($\delta_2 > \Delta$). Then,

$$P(\delta) > 0 \quad \Leftrightarrow \quad \delta < \delta_1 \text{ or } \delta > \delta_2.$$

Because $\delta > \delta_2 > \Delta$ is contrary to the hypothesis of §2.4.2,

$$P(\delta) > 0 \Leftrightarrow \delta < \delta_1 \text{ , that is } d_i < d_2 \Leftrightarrow \delta < \delta_1.$$

7. REFERENCES

[1] J. Astola, P. Haavisto, and Y. Neuvo. "Vector Median Filters". In *Proceedings of the IEEE*, volume 78-4, pages 678–689, April 1990.

[2] K. Öistämö and Y. Neuvo. "Video Signal Processing Using Vector Median". In *Proc. of VCIP'90*, pages 1171–1182, October 1990.

[3] I. Pitas and P. Tsakalides. "Multivariate Ordering in Color Image Filtering". *IEEE Tr. on Circuits and Systems for Video Technology*, 1(3):247–259, September 1991.

[4] T. Viero, K.O. Öistämö, and Y. Neuvo. "Three-Dimensional Median-Related Filters for Color Image Sequence Filtering". *IEEE Tr. on Circuits and Systems for Video Technology*, 4(2):129–142, April 1994.

Figure 8: R-G-B noisy test pattern : after mm, VML_1 and VML_2 filtering (resp. top, center and bottom).
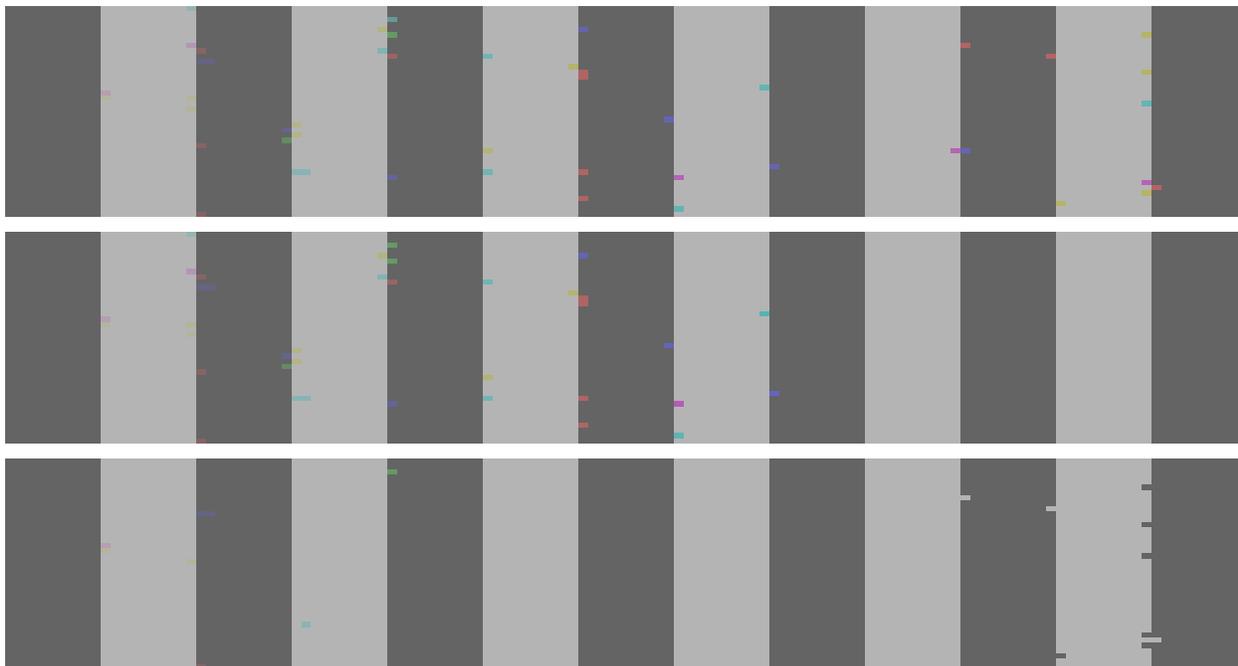

Figure 9: R-G-B noisy image, filtered by a 3∗3 marginal median (left) and by a 3∗3 VML_2 filter (right).

Figure 10: Y-U-V noisy image, filtered by a 3∗3 mm filter (left) and by a 3∗3 VML_2 filter (right).